Pure Appl. Chem., Vol. 83, No. 8, pp. 1515–1528, 2011.
doi:10.1351/PAC-CON-10-10-16

A graph-theoretical model for ballistic conduction in single-molecule conductors*

Patrick W. Fowler‡, Barry T. Pickup, and Tsanka Z. Todorova

Department of Chemistry, University of Sheffield, Sheffield S3 7HF, UK

Abstract: The tight-binding version of the source-and-sink potential (SSP) model of ballistic conduction can be cast in a graph-theoretical form where the transmission through a molecular wire depends on four characteristic polynomials: those of the molecular graph and the vertex-deleted subgraphs with one or both of the molecular vertices contacting the electrodes removed. This gives an explicit function for the dependence of transmission on energy, one that is well adapted for qualitative description of general classes of conductors and conduction behavior. It also leads directly to a selection-rule criterion for conduction in terms of counting zero roots of the polynomials, which for benzenoids and graphenes is shown to subsume literature approaches based on Kekulé structure counting, bond order, and frontier-orbital matching. As explicitly demonstrated here, the SSP transmission function agrees with that derived by the Green's function (GF) method.

Keywords: conduction; graph theory; molecular device; nanotechnology; selection rule.

INTRODUCTION

This article deals with a simplified description of ballistic conduction of electrons through single molecules. We envisage a conjugated molecule acting as a "molecular wire" that connects input and output reservoirs of electrons, c.f. Fig. 1. The molecule itself is connected to each reservoir by metallic wires, idealized as semi-infinite linear chains of atoms, and it is supposed that the wire-to-molecule contacts are made with atomic precision, between one atom of the molecule and the end atom of the chain. Two methods have been used to describe conduction in such devices. The first is the Green's function (GF) method [1], used widely in theoretical physics to describe a great variety of phenomena, including ionization and excitation processes, and transport phenomena, including electron scattering in metals. This method has also been used in the description of scanning tunneling microscopy. Application of this theory in a systematic way to the reservoir picture of molecular conduction is exemplified by the work of Ratner et al. [2].

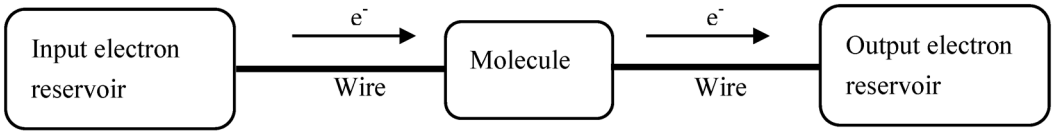

Fig. 1 Schematic representation of a molecular electronic device in the GF method.

*Paper based on a presentation made at the 20th International Conference on Physical Organic Chemistry (ICPOC-20), Busan, Korea, 22–27 August 2010. Other presentations are published in this issue, pp. 1499–1565.
‡Corresponding author

A recently introduced alternative methodology, the source-and-sink potential approach (SSP) [3–5] replaces the infinite connecting wires by single atoms on the left and right, c.f. Fig. 2, which act as source-and-sink atoms that introduce and remove the electron current. Non-Hermitian potentials are defined on the source-and-sink atoms to ensure that the correct scattering-theory boundary conditions are obeyed.

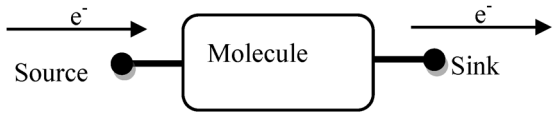

Fig. 2 Schematic representation of a molecular electronic device in the SSP method.

This is the method that has been used by the Sheffield group to formulate the graph-theoretical model of ballistic conduction [6–10] that will be discussed in the following three sections. It gives an explicit theoretical link between conduction, molecular structure, and patterns of connections, and suggests approximations and selection rules based on "chemical" concepts such as nonbonding orbitals, Kekulé structures, bond orders, and molecular orbital coefficients [9,10]. In view of the potential utility of the design principles that have been derived with the aid of the SSP formalism, it seems worth checking that they are not artifacts of the approach, and so the final section of the present article provides an explicit mathematical demonstration of the fact that both SSP and GF approaches lead to the same expression for the transmission function in the graph-theoretical tight-binding approximation.

THE SOURCE-AND-SINK POTENTIAL MODEL

The SSP method provides a phenomenological description of the process of ballistic conduction. It begins from a picture of the molecule as connected to semi-infinite wires, and asks for a stationary solution for the current under scattering boundary conditions: an incoming electron wave travels from infinity along the left wire, is partly transmitted into the molecule, and partly reflected from it at the left contact; the transmitted part of the wave exits the molecule at the right contact and travels off to infinity (c.f. Fig. 3).

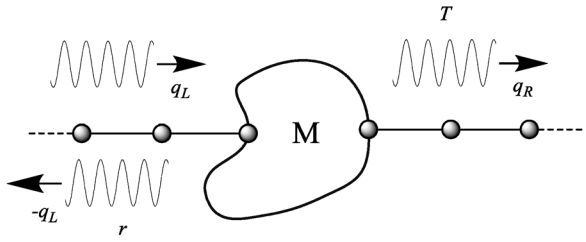

Fig. 3 Schematic representation of scattering of electron waves in a molecular electronic device.

Recognizing that the role of the wires is only to supply a fractional electron to the molecule from the left (and remove it at the right), the creators of the SSP model represent the parts of the device beyond the conducting molecule by fictitious source-and-sink vertices that carry non-Hermitian (complex) potentials designed to implement the boundary conditions [3–5]. When Hückel approximations are applied, the effective Hamiltonian matrix then consists of a molecular block describing the interactions amongst the N molecular centers, augmented by two rows and columns. These extra rows and

columns contain, in sparse off-diagonal positions, coupling elements between the source-and-sink vertices (L and R) and single connection sites in the molecule ($\bar{L}$ and $\bar{R}$), and in the diagonal positions the two complex potentials

$$a_L = \beta_L \frac{e^{-iq_L} + re^{iq_L}}{1+r} \tag{1}$$

and

$$a_R = \beta_R e^{-q_R} \tag{2}$$

where q_L and q_R are the wave vectors of the travelling waves in the left and right wires, defined in terms of the total energy and the respective coulomb and resonance integrals by

$$E = \alpha_L + 2\beta_L \cos q_L = \alpha_R + 2\beta_R \cos q_R \tag{3}$$

and r is the reflection coefficient, linked to the transmission by $T = 1 - |r|^2$. Both r and T are functions of energy, and the allowed energies are those of waves on the semi-infinite wires, given by $0 \le q_L, q_R \le \pi$. The full SSP Hamiltonian matrix in the standard choice where energies are referred to α, the coulomb integral for sites within the molecule, is

$$\mathbf{H}^{SSP} = \begin{pmatrix} \mathbf{A}\beta & \mathbf{e}_L\beta_{L\bar{L}} & \mathbf{e}_R\beta_{R\bar{R}} \\ \mathbf{e}_L^\dagger\beta_{L\bar{L}} & a_{LL} & 0 \\ \mathbf{e}_R^\dagger\beta_{R\bar{R}} & 0 & a_{RR} \end{pmatrix} \tag{4}$$

where $\beta_{L\bar{L}}$ and $\beta_{R\bar{R}}$ are resonance integrals coupling the source-and-sink atoms to the atoms $\bar{L}$ and $\bar{R}$ of the molecule, and the column vectors $\mathbf{e}_L$, $\mathbf{e}_R$ are each filled with zero entries apart from the one unit entry in rows $\bar{L}$ and $\bar{R}$, respectively. Given the simple dependence of the matrix on r, through the single $L\bar{L}$ element, the solution for r, T, and ultimately for the entries in the current-carrying eigenvector is easily obtained by setting the determinant $|E\mathbf{1} - \mathbf{H}^{\mathrm{SSP}}|$ to zero and expanding it along the sparse rows and columns. As shown in [6], the resulting expression for T(E) for the molecular device is

$$T(E) = \frac{4 \sin q_L \sin q_R (\tilde{u}\tilde{t} - \tilde{s}\tilde{v})}{\left| e^{-i(q_L+q_R)}\tilde{s} - e^{-iq_R}\tilde{t} - e^{-iq_L}\tilde{u} + v \right|^2} \tag{5}$$

where four polynomial functions of energy are defined for the molecule by

$$\begin{aligned} \tilde{s} &= \det|E\mathbf{1} - \mathbf{H}^M|, & \tilde{t} &= \tilde{\beta}_L \det|E\mathbf{1} - \mathbf{H}^M|^{\bar{L}\bar{L}}, \\ \tilde{u} &= \tilde{\beta}_R \det|E\mathbf{1} - \mathbf{H}^M|^{\bar{R}\bar{R}}, & \tilde{v} &= \tilde{\beta}_L\tilde{\beta}_R \det|E\mathbf{1} - \mathbf{H}^M|^{\bar{L}\bar{R},\bar{L}\bar{R}} \end{aligned} \tag{6}$$

with reduced parameters $\tilde{\beta}_L = \beta_{L\bar{L}}^2/\beta_L$ and $\tilde{\beta}_R = \beta_{R\bar{R}}^2/\beta_R$.

The superscript notation here is used to indicate the rows and columns struck out of the $n \times n$ determinant $|E\mathbf{1} - \mathbf{H}^{\mathrm{M}}|$, from which it is easily seen that each quantity is the (scaled) characteristic polynomial of a well-defined graph: respectively, the molecular graph, the molecular graph with $\bar{L}$ deleted, the molecular graph with $\bar{R}$ deleted and the molecular graph with both $\bar{L}$ and $\bar{R}$ deleted.

The product of sine functions acts as a band-pass filter, restricting the electron energy to the range of energies to the allowed wire states, and the parameter $\tilde{\beta}^2 = \tilde{\beta}_L\tilde{\beta}_R$ encapsulates all the physical parameters of the device through the relative values of the resonance integrals for the different types of contact. Although not apparent from the form in which it is written, the combination

$$(\tilde{u}\tilde{t} - \tilde{s}\tilde{v}) = (ut - sv)\,\tilde{\beta}^2$$

is a perfect square, as can be proved with the aid of Jacobi's theorem ([11], Appendix 2). One extremely useful feature of eq. 5 is that it leads to a simple, and purely graph-theoretical, necessary condition for conduction: for an energy within the allowed range, vanishing of $T(E)$ (opacity of the device or occurrence of an "anti-resonance") requires vanishing of the numerator. Hence, if $T(E) = 0$, then $(ut - sv) = 0$. The reverse implication does not hold: vanishing of $(ut - sv)$ for some energy E does not infallibly imply $T(E) = 0$, as the denominator may also vanish at the same energy, a fact that can sometimes cause confusion [12]. This important distinction between necessary and sufficient conditions can be exploited to derive selection rules for conduction, as will be shown below. In view of its important role in relation to opacity, the function $(ut - sv)$ has been called the opacity polynomial [8]. In the present article, this polynomial will be denoted by the symbol j^2 to make explicit its character as a square. Two applications based on the properties of the opacity polynomial are now discussed.

COMPOSITE DEVICES

The opacity polynomial j^2 is a purely graph-theoretical quantity. It depends on energy and on the pair of connections $\bar{L}$ and $\bar{R}$. The simplest example of its use is for P_n, the path on n vertices (the molecular graph of the linear polyene), connected end-to-end within a circuit. For this case

$$(ut - sv) = \varphi^2(P_{n-1}) - \varphi(P_n)\varphi(P_{n-2}) = 1 \tag{7}$$

where $\varphi(G)$ is the characteristic polynomial of graph G. The fact that the opacity polynomial is identically equal to the constant 1 means that the full transmission function has no zeroes, and is contained within the contour of the band-pass filter, modulated only by the variation with energy of the denominator in eq. 5. Analytical transmission functions for paths and cycles with general connections are given in [6].

Another infinite class of systems with easily computed opacity polynomials arises for "composite" devices, where the conducting molecule is built up from a set of "fragments" or repeating units, linked together in specific ways. Classical graph-theoretical theorems ([11], Chapter 4) about component graphs linked by a bridging edge (a bridging edge is one that when cut disconnects the molecular graph) can be used to predict the opacity polynomial and hence to recover the main part of the behavior of the transmission function from the spectral properties of their units. For example, two theorems proved in [8] relate to opacity polynomials of series devices consisting of (i) a string of units linked by bridging edges, and (ii) a string of units linked by a bridging edge to the vertices of a backbone, lollipop fashion (see Fig. 4). They are:

Theorem 1 (5 in [8]): The opacity polynomial of a series device G consisting of a sequence of units G_1-G_2-G_3-$\cdots$-G_N linked by bridging edges, as in Fig. 4a, with $\bar{L}$ in G_1 and $\bar{R}$ in G_N is

$$j^2(G) = \prod_{i=1}^{N} j^2(G_i) \tag{8}$$

where the individual opacity polynomials $j^2(G_i)$ are found by taking the ends of the bridging edges as contacts $\bar{R}$ for the unit to the left, and $\bar{L}$ for the unit to the right.

Theorem 2 (6 in [8]): The opacity polynomial of a series device G consisting of a backbone B, with attached lollipop side groups $H_1, H_2, \cdots H_N$, as in Fig. 4b, and with $\bar{L}$ and $\bar{R}$ in B is

$$j^2(G) = j^2(B)\prod_{i=1}^{N} \varphi^2(H_i) \tag{9}$$

The two theorems have physically important corollaries. For example, by Theorem 1, a series device will cease to conduct only at energies where one of the subunits G_i is opaque. By Theorem 2, opacities for a series device may be produced by interference effects caused by the side chains, as the overall opacity polynomial will vanish whenever the energy matches an eigenvalue for a side-chain molecular

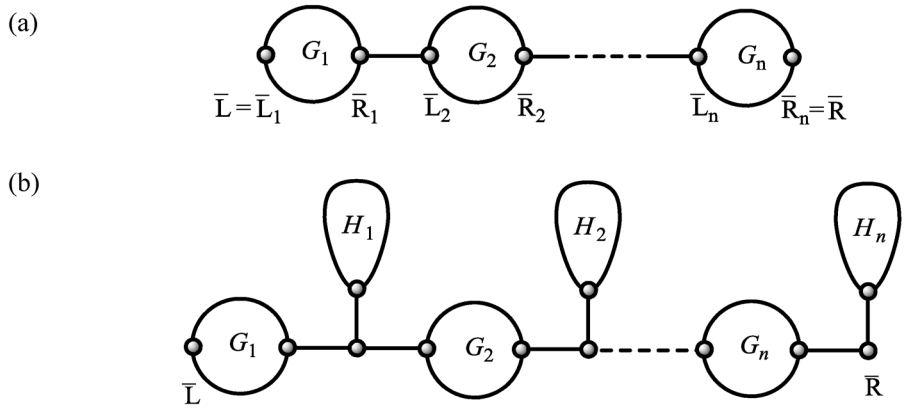

Fig. 4 Two types of composite device: (a) series connection of units through bridging edges; (b) connection of "lollipop" side-chain units via bridging edges to a backbone.

graph, with consequences for the overall current in the backbone, even though side chains of this type never support their own current, at this or any other energy. Side-chain effects have been noted in other treatments [13–15]; Theorem 2 shows that they are inevitable consequences of even the simplest quantum treatment.

Both theorems also have consequences for "polymer" devices as they show that increase in the number of repetitions of a backbone unit or a particular side chain both tend to broaden anti-resonances, as the point where $T(E) = 0$ becomes a minimum at which successively higher derivatives of T with respect to energy vanish, leading to a characteristic "scooped-out" region of vanishing transmission bounded by steep walls. An analogous mathematical effect of repeated multiplication of small numbers leads to local minima in the transmission spectra of small oligomers turning into similar scooped-out zeroes for longer and more heavily functionalized chains. Examples of both these qualitative trends are shown in Figs. 6–10 of [8].

SELECTION RULES, KEKULÉ STRUCTURES, AND BOND ORDERS

As noted above, the form of $T(E)$ as a ratio of square terms dictates a necessary condition for opacity. However, as both numerator and denominator are high-order polynomial functions, it is necessary to investigate more closely what may happen at energies where $(ut - sv)$ vanishes before concluding that $T(E)$ also vanishes. A key insight is given by the relationship of the sequences of polynomials s, t, v, and s, u, v as characteristic polynomials of graphs derived by successive deletion of vertices. Cauchy's interlacing theorem [16] applies to both sequences, and it places bounds on the eigenvalues of t and u in terms of those of s, and of v in terms of those of t and u. The behavior of $T(E)$ depends on whether E is a root of any or all of s, t, u, and v, and with what multiplicity. Writing

$$\begin{aligned} s &= E^{g_s}\, s'(E) \\ t &= E^{g_t}\, t'(E) \\ u &= E^{g_u}\, u'(E) \\ v &= E^{g_v}\, v'(E) \end{aligned} \tag{10}$$

where s', t', u', v' are all non-zero at $E = 0$, it can be shown [9] from interlacing that there are 11 realizable cases for the multiplicity combination g_s, $g_t \geq g_u$, g_v. These comprise five where $T(0) = 0$, five where $T(0) \neq 0$, and one where $T(0) = 0$ if and only if $[u'(0)\, t'(0) - s'(0)\, v'(0)] = 0$. The criteria for opacity/conduction can be condensed to three *selection rules* based on comparing numbers of zero roots. They are [9]:

(1) For *bipartite* graphs G, the system conducts at the Fermi level if and only if

$$g_s = g_v \text{ and } g_t = g_u \tag{11}$$

(which in fact implies $g_t = g_s \pm 1$).

(2) For *non-bipartite* graphs G, with the four multiplicities g_s, g_t, g_u, g_v not all equal, the system conducts at the Fermi level if and only if

$$\min [(g_s + g_v)/2, (g_t + g_u)/2] = \min [g_s, g_t, g_u, g_v] \tag{12}$$

(3) For *non-bipartite* graphs G, with all four multiplicities g_s, g_t, g_u, g_v equal, the system conducts at the Fermi level if and only if

$$u'(0)\, t'(0) - s'(0)\, v'(0) = 0 \tag{13}$$

(In the degenerate case of "ipso" connection, where left and right contact atoms are the same, the rules reduce to the statement that the device is opaque, conducting or fully transparent, as $g_t = g_s + 1$, g_s or $g_s - 1$, respectively.)

Only in the special case of equal multiplicities for all four polynomials is it necessary to make a detailed calculation based on the tail coefficients of the four polynomials, or equivalently on the products of their non-zero roots. These rules are already simple and easy to apply. For example, the three cases of connection of benzene in *ortho*, *meta*, and *para* connection patterns all have $g_s = 0$, $g_t = g_u = 1$, but have $g_v = 0$, 2, and 0, respectively, and hence by rule 1 the *ortho* and *para* connections conduct at $E = 0$ but *meta* does not [9,6].

However, perhaps the main interest of the rules is that they tie together the many different approaches to rules of thumb for prediction of conduction. The links are most easily seen if we restrict attention to benzenoids (i.e., molecular graphs that are simply connected fragments of the graphene plane) that are connected via perimeter vertices. These graphs are bipartite and hence covered by selection rule 1. A benzenoid is said to be Kekulean if it has a perfect matching, i.e., an assignment of formal single and double bonds such that every carbon atom is included in exactly one double bond. Clearly, all Kekulean benzenoids have even n. For a benzenoid and the derived graphs for perimeter connections [10] (and see [17,18]), there is a simple relation between the tail coefficient of the characteristic polynomial φ (G) and the number of Kekulé structures, K, i.e.,

$$(-)^{n/2}\, K^2 = \varphi\,(0)$$

There are three possibilities: G is Kekulean, or G has an odd number of vertices but at least one of G-$\overline{L}$ and G-$\overline{R}$ is Kekulean, or all three of G, G-$\overline{L}$, and G-$\overline{R}$ are non-Kekulean. The first two possibilities lead to simple expressions for transmission in terms of Kekulé counts K_s, K_t, K_u, and K_v for the four graphs. When G is Kekulean, we have

$$T(0) = 4K_s^2\, K_v^2 \tilde{\beta}^2/(K_s^2 + K_v^2 \tilde{\beta}^2)^2 \tag{14}$$

and since $K_s \neq 0$, this implies $T(0) \neq 0$ if and only if $K_v \neq 0$, conduction is allowed if and only if the molecular graph remains Kekulean on deletion of the two contact vertices. When G itself is a benzenoid with an odd number of atoms but at least one of G-$\overline{L}$ and G-$\overline{R}$ is Kekulean, we have

$$T(0) = 4K_t^2\, K_u^2/(K_t^2 + K_u^2)^2 \tag{15}$$

and so conduction occurs at the Fermi level if and only if both G-$\overline{L}$ and G-$\overline{R}$ are Kekulean. The third case is more complicated as the lack of Kekulé structures implies that g_s, g_t, and g_u are all non-zero. Falling back on selection rule 1, we see that we must have $g_s = g_v$ and $g_t = g_u$, and then the transmission can be calculated from tail coefficients of the reduced characteristic polynomials as

$$\text{for } g_t = g_s + 1 \qquad T(0) = -4s'(0)v'(0)\tilde{\beta}^2/(s'(0) - v'(0)\tilde{\beta}^2)^2 \tag{16}$$

$$\text{for } g_t = g_s - 1 \qquad T(0) = -4u'(0)t'(0)/(u'(0) + t'(0))^2 \tag{17}$$

and $T(0) = 0$ otherwise.

This description in terms of Kekulé structures leads neatly to a connection with the picture of conduction in graphene fragments in terms of Pauling long-bond orders [19]. The usual Pauling bond order is defined for a pair of adjacent atoms as the fraction of the Kekulé structures that contain a double bond linking that pair. In the generalization [19], the Pauling bond order is defined for any pair, adjacent or otherwise, as the ratio of the Kekulé count for the structure with the two atoms deleted to the original Kekulé count, i.e., K_s/K_v in our terms. Therefore, for a Kekulean benzenoid, eq. 14 translates to

$$T(0) = 4P^2_{\bar{L}\bar{R}}\,\tilde{\beta}^2/(1 + P^2_{\bar{L}\bar{R}}\,\tilde{\beta}^2) \tag{18}$$

where $P_{\bar{L}\bar{R}}$ would be the Pauling bond order of a "long bond" imagined to be inserted between the left and right contact atoms. This corresponds to the criterion applied by Klein and co-workers in [19] that requires a non-zero long-bond order for conduction at the Fermi level, but the present formula carries an extra level of detail in that it shows that such conduction is not monotonically dependent on the bond order: $T(0)$ is an increasing function of K_v for the range

$$0 \le P_{\bar{L}\bar{R}} \le \tilde{\beta}^{-1} \tag{19}$$

but for larger values of K_v the transmission begins to tail off with increasing numbers of perfect matchings in the double vertex-deleted graph [10].

Likewise [10], the expression for transmission in the case of a non-Kekulean benzenoid with Kekulean vertex-deleted subgraphs can be cast in terms of generalized Pauling spin densities. We define P_{a} as the fraction of maximum matchings of G that leave vertex a unmatched (i.e., otherwise complete Kekulé structures in which a is one of the minimum number of sites unavoidably left with an unpaired electron). In such a case, eq. 15 translates to

$$T(0) = \frac{4P^2_{\bar{L}}P^2_{\bar{R}}}{\left(P^2_{\bar{L}} + P^2_{\bar{R}}\right)} \tag{20}$$

which requires non-zero Pauling spin density on both contacts and gives the maximum (perfect) transmission when the two spin densities are equal, as for example when the contact atoms are equivalent by symmetry.

A further connection can be made with the molecular orbital picture, and specifically with the frontier orbital rule of thumb for conduction. The linking concept is the Ruedenberg bond order, which for a pair of centers a and b is the weighted sum over occupied orbitals of the product of coefficients on the two centers [20]

$$R_{\bar{L}\bar{R}} = \sum_k n_k c^{(k)}_{\bar{L}} c^{(k)}_{\bar{R}} \Big/ \varepsilon_k \tag{21}$$

where n_k is the occupation number, and ε_k is the orbital energy of the k^{th} molecular orbital. Kekulean benzenoids have no nonbonding orbitals, and for them the Pauling and Ruedenberg definitions of bond order give identical results for pairs of neighbors [21] and results of identical magnitude [22] for other pairs where the two atoms are in different partite sets. The case where both members of the pair belong to the same partite set is not of interest, as then $K_v = 0$ and there is no transmission, by eq. 14.

The frontier orbital criterion for conduction in benzenoids is based on a perturbed GF approach, which considers conduction in the limit of weak coupling between the molecule and the wires. In this limit, the transmission for a Kekulean benzenoid where the contact vertices are in different partite sets is

$$T(0) = 4P^2_{\bar{L}\bar{R}}\,\tilde{\beta}^2 = 4R^2_{\bar{L}\bar{R}}\,\tilde{\beta}^2 \approx C\,[c^{\mathrm{HOMO}}_{\bar{L}}\,c^{\mathrm{HOMO}}_{\bar{R}}]^2 \tag{22}$$

where C is a constant and the final approximate equality follows by assuming that the Ruedenberg bond order and hence conduction will be dominated by the term arising from the orbital with the smallest orbital energy, i.e., from the highest occupied molecular orbital (HOMO). This gives a simple rule of thumb for conduction pathways: the two contact vertices should have a large-magnitude product of coefficients in the HOMO that changes sign in the lowest unoccupied molecular orbital (LUMO) [23]. Interestingly, the interaction could be either strongly bonding or strongly antibonding. The approximate eq. 22 does appear to pick out strongly conducting connection patterns in many cases, though at a quantitative level, the correlation with the full eq. 5 is patchy [10]. If the HOMO is degenerate, the coefficient term should be summed over all orbitals in the degenerate set. The term approximated in eq. 22 is just the first of a perturbation series: a more detailed perturbation theory of transmission can be built up in terms of orbital densities and their response functions [24].

In the next section of the paper, we turn from the deductions that can be made from the SSP model to the question of whether the same results would follow from the more widely used GF formulation.

THE GREEN'S FUNCTION APPROACH

The Hamiltonian for the GF model is written in [2] as

$$H = H^{(0)} + V \tag{23}$$

where the zeroth order Hamiltonian

$$H^{(0)} = \sum_l \varepsilon_l^{(0)} |l\rangle\langle l| + \sum_{m=1}^{N} \varepsilon_m^{(0)} |\phi_m\rangle\langle\phi_m| + \sum_r \varepsilon_r^{(0)} |r\rangle\langle r| \tag{24}$$

has three terms, the first being a sum over the eigenstates of the electrons, l, in the left wire, the second is over the N atomic sites of the molecule. In our straightforward Hückel theory model, as before, we set $\varepsilon_m^{(0)} = \alpha \equiv 0$, and take φ as an atomic orbital on molecular site m. The final term in eq. 24 is a sum over the eigenstates, r, of the electrons in the right-hand wire.

The eigenstates of the wires are defined using Hückel theory for a linear chain of N atoms. At a later stage it will be necessary to take the limit as $N \to \infty$. Hence, we will write the left wire states as

$$|l\rangle = \sqrt{\frac{2}{N+1}} \sum_{i=1}^{N} \sin\left[\pi il/N+1\right] \left|\phi_i^{\text{left}}\right\rangle,\ \varepsilon_l^{(0)} = \alpha_L + 2\beta_L \cos\left[\pi il/N+1\right] \tag{25}$$

where ϕ_i^{left} is on atomic site i on the left wire, and the wire eigenstates lie in an energy band of width $2\beta_L$, centered about the energy α_L. There is an analogous equation for the right wire with wire eigenstates in an energy band of width $2\beta_R$, centered about the energy α_R.

The "interaction" Hamiltonian, which describes the couplings between the three parts of the device

$$V = \left(\sum_l V_{l\bar{L}} |l\rangle\langle\phi_{\bar{L}}| + \sum_r V_{r\bar{R}} |r\rangle\langle\phi_{\bar{R}}| + \text{adjoint} \right) + \sum_{m\sim n} H_{mn}^{M} |\phi_m\rangle\langle\phi_n| \tag{26}$$

also has three terms, the first two of which are couplings between the left and right wires and single connection sites in the molecule, $\bar{L}$ and $\bar{R}$. The choice of single left- and right-hand connection atoms makes the model simpler; generalizations will require more terms in the Hamiltonian. The final set of terms in eq. 26 consists of summations over connected atoms, and for a pure carbon skeleton we will set $H_{mn}^{M} = \beta\delta_{mn}$, where δ_{mn} is unity if the atoms are connected, and zero otherwise. The terms coupling the left hand wire to the molecule are defined so that the left wire contact to the atom $\bar{L}$ is the first atom of the chain, numbering from right to left away from the molecule. Similarly, we shall number the right-hand wire starting with the first atom as the one in contact with $\bar{R}$. With these definitions we can define the coupling terms in eq. 26 as

$$V_{l\bar{L}} = \langle l|V|\phi_{\bar{L}}\rangle = \beta_{L\bar{L}}\sqrt{\frac{2}{N+1}}\sin\left(\frac{l\pi}{N+1}\right),\ V_{r\bar{R}} = \langle r|V|\phi_{\bar{R}}\rangle = \beta_{R\bar{R}}\sqrt{\frac{2}{N+1}}\sin\left(\frac{r\pi}{N+1}\right) \tag{27}$$

which have unique resonance integrals β for the wire-molecule contact interactions.

In the GF approach [2], the conductance can be written as

$$g = \frac{2\pi e^2}{\hbar}\left|G_{\bar{L}\bar{R}}(E)\right|^2 \sum_l \left|V_{l\bar{L}}\right|^2 \delta(\varepsilon_l^{(0)} - E_F)\sum_r \left|V_{r\bar{R}}\right|^2 \delta(\varepsilon_r^{(0)} - E_F) \tag{28}$$

where E_F is the Fermi energy, and the GF matrix element is

$$G_{\bar{L}\bar{R}}(E) = (E\mathbf{1} - \mathbf{H})^{-1}_{\bar{L}\bar{R}} \tag{29}$$

In eq. 29, we have changed to a matrix representation based on sites in the molecule, where the Hamiltonian matrix in block form is

$$\mathbf{H} = \begin{pmatrix} E\mathbf{1} - \mathbf{H}^M & -\mathbf{V}_L & -\mathbf{V}_R \\ -\mathbf{V}_L^\dagger & E\mathbf{1} - \boldsymbol{\varepsilon}_L^{(0)} & \mathbf{0} \\ -\mathbf{V}_R^\dagger & \mathbf{0} & E\mathbf{1} - \boldsymbol{\varepsilon}_R^{(0)} \end{pmatrix} \tag{30}$$

where $(\boldsymbol{\varepsilon}_L^{(0)})_{ll'} = \delta_{ll'}\varepsilon_l^{(0)}$, $(\boldsymbol{\varepsilon}_R^{(0)})_{rr'} = \delta_{rr'}\varepsilon_r^{(0)}$ are diagonal matrices indexed by the states of the wires, and the coupling matrices $(\mathbf{V}_L)_{ml} = \delta_{m\bar{L}}\beta_{L\bar{L}}V_{l\bar{L}}$, $(\mathbf{V}_R)_{mr} = \delta_{m\bar{R}}\beta_{R\bar{R}}V_{r\bar{R}}$ in terms of the matrix elements defined in eq. 27.

The GF matrix

$$\mathbf{G}(E)^{-1} = E\mathbf{1} - \mathbf{H}^M - \mathbf{V}_L\,(E\mathbf{1} - \boldsymbol{\varepsilon}_L^{(0)})^{-1}\,V_L^\dagger - \mathbf{V}_R\,(E\mathbf{1} - \boldsymbol{\varepsilon}_R^{(0)})^{-1}\,V_R^\dagger \tag{31}$$

can be simplified using the fact that the wire Hamiltonians are diagonal. Hence, using the left-hand connection as an example

$$\left[\mathbf{V}_L(E\mathbf{1} - \boldsymbol{\varepsilon}_L^{(0)})^{-1}\mathbf{V}_L^\dagger\right]_{mm'} = \delta_{m\bar{L}}\delta_{m'\bar{L}}\beta_{L\bar{L}}^2\frac{2}{N+1}\sum_{l=1}^{N}\frac{\sin^2\left(l\pi/N+1\right)}{E - \alpha_L - 2\beta_L\cos\left(l\pi/N+1\right)} \tag{32}$$

The simplification of the right-hand-side of eq. 32 is detailed in Appendix A, and we can deduce that eq. 31 becomes

$$\mathbf{G}(E)^{-1} = E\mathbf{1} - \mathbf{H}^M - \delta_{m\bar{L}}\delta_{m'\bar{L}}\tilde{\beta}_L\,e^{-iq_L} - \delta_{m\bar{R}}\delta_{m'\bar{R}}\tilde{\beta}_R\,e^{-iq_R} \tag{33}$$

where we have defined energy scaling parameters as in eq. 6.

Equation 33 is almost the characteristic matrix for the molecular system in the Hückel approximation except that terms have been added to the diagonal of the matrix for the two contact atoms.

It is useful to express GF via the standard formula for a matrix inverse

$$\mathbf{G}_{\bar{L}\bar{R}}(E) = (-)^{\bar{L}\bar{R}}\det|E\mathbf{1} - \mathbf{H}|^{\bar{L}\bar{R}}/\det|E\mathbf{1} - \mathbf{H}| \tag{34}$$

where the superscript on the determinant in the numerator implies that row $\bar{L}$ and column $\bar{R}$ have been removed. We define the characteristic polynomial

$$(-)^{\bar{L}\bar{R}}\sqrt{\tilde{\beta}_L\tilde{\beta}_R}\,\det\left|E\mathbf{1} - \mathbf{H}\right|^{\bar{L}\bar{R}} = (-)^{\bar{L}\bar{R}}\sqrt{\tilde{\beta}_L\tilde{\beta}_R}\,\det\left|E\mathbf{1} - \mathbf{H}^M\right|^{\bar{L}\bar{R}} = \tilde{j}_{\bar{L}\bar{R}} \tag{35}$$

which is dependent only upon the properties of the molecule.

The simplification of the "density of states" terms in eq. 28 is described in Appendix B.

The denominator of eq. 33 is simplified by expanding in terms of the extra elements added to the diagonal. Using the definitions of the characteristic polynomials in eq. 6

$$\det|E\mathbf{1} - \mathbf{H}| = \tilde{s} - e^{-iq_L}\,\tilde{t} - e^{-iq_R}\,\tilde{u} + e^{-iq_L}\,e^{-iq_R}\,\tilde{v} \tag{36}$$

so that the final formula for the conduction is

$$g = \frac{e^2}{h}\frac{4\tilde{j}^2_{L\bar{R}}\sin q_L \sin q_R}{\left|\tilde{s} - e^{-iq_L}\tilde{t} - e^{-iq_R}\tilde{u} + e^{-iq_L}e^{-iq_R}\tilde{v}\right|^2} \tag{37}$$

where

$$\tilde{j}^2_{L\bar{R}} = \tilde{u}\tilde{t} - \tilde{s}\tilde{v} \tag{38}$$

is the opacity polynomial of previous sections, and the expression for g is compatible with both eqs. 28 and 5, demonstrating the exact equivalence of GF and SSP.

CONCLUSION

This paper has considered some graph-theoretical aspects of the SSP model of ballistic conduction and has shown that it is fully compatible with the GF approach. The specific formulation of the transmission function in terms of characteristic polynomials has several advantages for revealing generic types of conduction behavior, and for making links to the various chemical models of conduction in terms of VB and MO ideas. Apart from those discussed here, the graph-theoretical approach has many more potential applications in which global behavior of whole classes of systems can be examined. For example, the fact that non-isomorphic conjugated Hückel systems may share the same characteristic polynomial and hence the same set of energy eigenvalues prompts the question of whether two non-isomorphic devices could have identical transmission functions, $T(E)$. The answer turns out to be in the affirmative, as demonstrated in detail in [7], and these model results have already prompted an investigation with more sophisticated methods to see how far these graph theoretical results carry over to "real" molecules and devices [25].

ACKNOWLEDGMENTS

TZT thanks the University of Sheffield for financial support and PWF thanks the Royal Society/Wolfson Scheme for a Research Merit Award during the tenure of which part of this work was carried out.

REFERENCES

1. E. N. Economou. Green's Functions in Statistical Physics, Springer, Berlin (1990).
2. (a) V. Mujica, M. Kemp, M. A. Ratner. *J. Chem. Phys.* **101**, 6849 (1994); (b) V. Mujica, M. Kemp, M. A. Ratner. *J. Chem. Phys.* **101**, 6856 (1994).
3. F. Goyer, M. Ernzerhof, M. Zhuang. *J. Chem. Phys.* **126**, 144104 (2007).
4. M. Ernzerhof. *J. Chem. Phys.* **127**, 204709 (2007).
5. P. Rocheleau, M. Ernzerhof. *J. Chem. Phys*. **130**, 184704 (2009).
6. B. T. Pickup, P. W. Fowler. *Chem. Phys. Lett.* **459**, 198 (2008).
7. P. W. Fowler, B. T. Pickup, T. Z. Todorova. *Chem. Phys. Lett.* **465**, 142 (2008).
8. P. W. Fowler, B. T. Pickup, T. Z. Todorova, T. Pisanski. *J. Chem. Phys.* **130**, 174708 (2009).
9. P. W. Fowler, B. T. Pickup, W. Myrvold, T. Z. Todorova. *J. Chem. Phys.* **131**, 044104 (2009).
10. P. W. Fowler, B. T. Pickup, T. Z. Todorova, W. Myrvold. *J. Chem. Phys*. **131**, 244110 (2009).

11. I. Gutman, O. E. Polyansky. *Mathematical Concepts in Organic Chemistry*, Springer, Berlin (1986).
12. T. Markussen, R. Stadler, K. S. Thygesen. *Nanoletters.* doi:10.1021/nl101688a
13. M. Ernzerhof, M. Zhuang, P. Rocheleau. *J. Chem. Phys.* **123**, 134704 (2005).
14. G. C. Solomon, D. Q. Andrews, R. P. van Duyne, M. A. Ratner. *Chem. Phys. Chem.* **10**, 257 (2009).
15. T. Hansen, G. C. Solomon, D. Q. Andrews, M. A. Ratner. *J. Phys. Chem*. **131**, 257 (2009).
16. A. L. Cauchy. In *Oeuvres Complètes d'Augustin Cauchy*, Paris: Gauthier-Villars et fils, 1882–1974, (IIe Série) Tome 9, p. 174, Exer. de math. 4 (1829).
17. H. Sachs. *Publ. Math. (Debrecen)* **11**, 119 (1964).
18. S. Fajtlowicz, P. John, H. Sachs. *Croat. Chem. Acta* **78**, 195 (2005).
19. T. Morikawa, S. Narita, D. J. Klein. *Chem. Phys. Lett*. **402**, 554 (2005).
20. N. S. Ham, K. Ruedenberg. *J. Chem. Phys*. **29**, 1215 (1958).
21. N. S. Ham. *J. Chem. Phys*. **29**, 1229 (1958).
22. E. Heilbronner. *Helv. Chim. Acta* **155**, 1722 (1962).
23. K. Yoshizawa, T. Tada, A. Staykov. *J. Am. Chem. Soc*. **130**, 9406 (2008).
24. P. Rocheleau, M. Ernzerhof. *J. Chem. Phy*s. **130**, 184704 (2009).
25. Y. X. Zhou, M. Ernzerhof. *J. Chem. Phy*s. **132**, 104706 (2010).

APPENDIX A

Taking the limit of eq. 32 as $N \to \infty$, converting the sum to an integral, and substituting $\theta = l\pi/(N+1)$, it becomes

$$\left[\mathbf{V}_L(E\mathbf{1}-\boldsymbol{\varepsilon}_L^{(0)})^{-1}\mathbf{V}_L^{\dagger}\right]_{mm'} = \delta_{m\bar{L}}\delta_{m'\bar{L}}\beta_{L\bar{L}}^2\frac{1}{\pi}\int_{-\pi}^{\pi}\frac{\sin^2\theta}{E-\alpha_L-2\beta_L\cos\theta}d\theta \tag{A1}$$

The right-hand side can be transformed into a contour integral in the complex plane, by making the substitution $\omega = \exp(i\theta)$

$$\delta_{m\bar{L}}\delta_{m'\bar{L}}\frac{\beta_{L\bar{L}}^2}{\beta_L}\frac{1}{2\pi i}\frac{1}{2}\oint_C d\omega\,\frac{\left(\omega-\omega^*\right)^2}{\omega^2-2\rho_L\omega+1} \tag{A2}$$

where we have defined a scaled energy $\rho_L = (E-\alpha_L)/2\beta_L$. The contour, C, is an anticlockwise contour around the unit circle in the complex plane.

We define an integral

$$S(\rho) = \frac{1}{2\pi i}\frac{1}{2}\oint_C d\omega\,\frac{(\omega-\omega^*)^2}{\omega^2-2\rho\omega+1} \tag{A3}$$

This integral can be simplified by expanding the square in the numerator of the integrand. It is easy to show that

$$\frac{1}{2\pi i}\frac{1}{2}\oint_C d\omega\,\frac{\omega^2}{\omega^2-2\rho\omega+1} = \frac{1}{2\pi i}\frac{1}{2}\oint_C d\omega\,\frac{\omega^{*2}}{\omega^2-2\rho\omega+1} \tag{A4}$$

so that eq. A3 becomes

$$S(\rho) = \frac{1}{2\pi i}\oint_C d\omega\,\frac{(\omega^2-1)}{\omega^2-2\rho\omega+1} = \frac{1}{2\pi i}\oint_C d\omega\,\frac{(\omega^2-1)}{(\omega-\rho_+)(\omega-\rho_-)} \tag{A5}$$

with

$$\rho_\pm = \rho \pm \sqrt{\rho^2-1} \tag{A6}$$

and where the roots satisfy $\rho_+\rho_- = 1$, $\rho_+ + \rho_- = 2\rho$. This form of the integral is appropriate for the use of the Cauchy residue theorem. We are primarily interested in real values of the scaled energy, ρ, and there are three cases to consider.

(i) $\rho > 1$

In this case, the roots (eq. A6) are real, and $|\rho_+| > 1$ is outside the contour, whilst $|\rho_-| < 1$ is inside. Hence

$$S(\rho) = \frac{\rho_-^2-1}{\rho_- - \rho_+} = \rho_- = \rho - \sqrt{\rho^2-1} \tag{A7}$$

(ii) $\rho < 1$

In this case, the roots (eq. A6) are real, and $|\rho_-| > 1$ is outside the contour, whilst $|\rho_+| < 1$ is inside. Hence

$$S(\rho) = \frac{\rho_+^2 - 1}{\rho_+ - \rho_-} = \rho_+ = \rho + \sqrt{\rho^2 - 1} \tag{A8}$$

(iii) $-1 \leq \rho \leq 1$

In this case, the roots are complex, and

$$\rho_\pm = \rho \pm i\sqrt{1-\rho^2} \tag{A9}$$

This case is illustrated in Fig. A1.

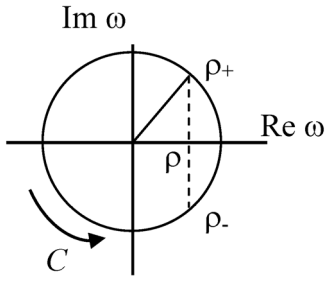

Fig. A1 The unit circle contour C.

The two roots are both on the contour, so it is necessary to add or subtract an infinitesimal imaginary value to the energy E in order to define the integral properly. We use $\eta = 0^+$, and deduce

$$S(\rho + i\eta) = \rho - i\sqrt{1-\rho^2} = e^{-iq} \tag{A9}$$

Since the positive imaginary part lifts ρ just outside the contour, whilstis inside. In eq. A8, we have used the bounds on ρ to define $q = \arccos(\rho)$. Similarly, it is easy to derive

$$S(\rho - i\eta) = \rho + i\sqrt{1-\rho^2} = e^{iq} \tag{A10}$$

APPENDIX B

The simplification of the density of states terms in eq. 28 uses the same manipulations as detailed n appendix A. Hence, using the left-hand connection as an example

$$\sum_l \left|V_{l\bar{L}}\right|^2 \delta(\varepsilon_l^{(0)} - E_F) = \beta_{L\bar{L}}^2 \frac{2}{N+1} \sum_{l=1}^{N} \sin^2\left(l\pi/N+1\right) \delta\left(E_F - \alpha_L - 2\beta_L \cos\left(l\pi/N+1\right)\right) \tag{B1}$$

and taking the limit $N \to \infty$ and making substitutions as before, we obtain

$$\sum_l \left|V_{l\bar{L}}\right|^2 \delta(\varepsilon_l^{(0)} - E_F) = \beta_{L\bar{L}}^2 \frac{1}{\pi} \int_{-\pi}^{\pi} \sin^2\theta \delta\left(E_F - \alpha_L - 2\beta_L \cos\theta\right) d\theta \tag{B2}$$

For a non-zero scale variable α, the delta function satisfies

$$\int_{-\infty}^{\infty} \delta(\alpha x) dx = \int_{-\infty}^{\infty} \delta(u) \frac{du}{|\alpha|} = \frac{1}{|\alpha|} \tag{B3}$$

so that we can deduce that

$$\sum_l \left|V_{l\bar{L}}\right|^2 \delta(\varepsilon_l^{(0)} - E_F) = \tilde{\beta}_L \frac{1}{2\pi} \int_{-\pi}^{\pi} \sin^2\theta \delta\left(\rho_L - \cos\theta\right) d\theta \tag{B4}$$

For a smooth continuously differentiable function, $g(x)$

$$\delta(g(x)) = \sum_i \frac{\delta(x - x_i)}{|g'(x_i)|} \tag{B5}$$

where the summation is over the all the roots, x_i, of $g(x)$. If we put

$$\rho_L = \cos q_L$$

as in appendix A, then we can recognize that the function

$$\cos q_L - \cos \theta$$

has roots

$$\theta = \pm q_L$$

and hence

$$\sum_l \left|V_{l\bar{L}}\right|^2 \delta(\varepsilon_l^{(0)} - E_F) = \frac{\tilde{\beta}_L}{\pi} \sin q_L \tag{B6}$$

